Bioorganic & Medicinal Chemistry Letters 30 (2020) 127288

Contents lists available at ScienceDirect

Bioorganic & Medicinal Chemistry Letters

journal homepage: www.elsevier.com/locate/bmcl

Potent dual EGFR/Her4 tyrosine kinase inhibitors containing novel (1,2-dithiolan-4-yl)acetamides

Tarek S. Mansour[a,*], Ranga R. Pallepati[b], Vishnu Basetti[b]

[a] Sabila Biosciences LLC, 5 Overlook Road, New City, NY 10956 USA
[b] Aurigene Discovery Technology Ltd. Bollaram Road, Miyapur, Hyderabad, 500 049 Telangana, India

ARTICLE INFO

Keywords:
EGFR
Her4
Cyanoquinolines
2-(1,2-dithiolan-4-yl)acetic acid
Homoasparagusic acid
Glycerol
Hollow fiber assay
MOLT4
H460
NCI-60

ABSTRACT

Modifications at C_6 and C_7 positions of 3-cyanoquinolines **6** and **7** led to potent inhibitors of the ErbB family of kinases particularly against $EGFR^{WT}$ and Her4 enzymes in the radioisotope filter binding assay. The lead (**4**, SAB402) displayed potent dual biochemical activities with $EGFR^{WT}$/Her4 IC_{50} ratio of 80 due to its potent inhibition of Her4 activity (IC_{50} 0.03 nM), however, the selectivity towards activating mutations ($EGFR^{L858R}$, $EGFR^{ex19del}$) was decreased. Inhibitor **4** also exhibited excellent growth inhibition in seven different cancer types and reduced cell viability in female NMRI nude mice in the intraperitoneally implanted hollow fibers which have been loaded with MOLT-4 (leukemia) and NCI-H460 (NSCLC) cells in a statistically significant manner.

The EGFR family consists of four members (ErbB1-4) of receptor tyrosine kinases that play a central role in signal transduction and are implicated in the pathogenesis of many cancers including non-small cell lung (NSCLC) and breast cancers.[1] Recently, we reported on our initial lead generation efforts of a series of 3-and 4-substituted 1,2 dithiolanes with lead candidates **1** and **2** emerging having good activities in NSCLC and leukemia cell lines.[2] The structure–activity relationship (SAR) studies have suggested that a methylene spacer between the (1,2-dithiolan-3-yl) moiety in **1** and **2** and the core heterocyclic structure was optimal and is preferred to longer or shorter homologs.[2] We also discovered that the biochemical activity is enhanced when the C_7 alkoxy substituent is replaced by 2,3-dihydroxy-propoxy moiety, derived from glycerol, and that a modest 2–3 fold preference favors of the *S* stereoisomer **3** (Fig 1). It was, therefore, deemed of relevance to target analogs of **3** such as **4** and **5** (Fig. 2) incorporating a methylene spacer between the (1,2 dithiolan-4-yl) moiety and the heterocyclic quinoline ring.

These analogs would be best prepared by a direct coupling of 6-amino 3-cyanoquinolines[2] **6** and **7** with 2-(1,2-dithiolan-4-yl)acetic acid **8** as previously demonstrated. However, acid **8** is a novel compound that has not been reported in the literature, and is a higher homolog of asparagusic acid (homoasparagusic acid). In this letter, we report on a practical synthesis of **8** from readily available starting material, and its subsequent coupling with 6-amino 3-cyanoquinolines **6** and **7** to afford target compounds **4** and **5**. The biological evaluation including biochemical, cellular and in vivo activities will be reported.

Our strategy to access **8** was based on preparing an appropriate acyclic 1,3 dithiol amenable to disulfide formation by an oxidative process. Towards this goal, the displacement reaction of 1,3-dichloropropan-2-one **9** with benzyl mercaptan under basic conditions afforded the bis-(benzylthio)propan-2-one **10** in 44% isolated yield. Wittig reaction of **10** with ethyl 2-(triphenylphosphanylidene)acetate proceeded smoothly to furnish the but-2-enoate ester **11** in 81% yield. Reduction of ester **11** to butanoate **12** was achieved with sodium borohydride-nickel chloride reagents in methanol-tetrahydrofuran solvent system at room temperature. Ester **12** was then, hydrolyzed under basic conditions to butanoic acid **13**. This, in turn, was subjected to a one pot reduction step in liquid ammonia followed by evaporation of ammonia and dissolving in aqueous toluene then oxidation with a gentle stream of oxygen to afford homoasparagusic acid **8** in 85% yield (5 steps from **9**, 10% overall yield) as shown in scheme 1.

With acid **8** in hand, coupling of each of **6** and **7** was mediated by *N*-(3-dimethylaminopropyl)-*N*'-ethylcarbodiimide hydrochloride (EDC) in *N*-methylpyrrolidone at 90 °C. The use of *ca.* 10 fold excess of **8** was necessary to produce acetonides **14** and **15** respectively, after preparative HPLC purification in modest yields. Hydrolysis of acetonides **14** and **15** furnished the target compounds **5** and **4** respectively, in good yields as depicted in Scheme 2.

* Corresponding author.
E-mail address: tsmansour@sabilabiosciences.com (T.S. Mansour).

https://doi.org/10.1016/j.bmcl.2020.127288
Received 16 March 2020; Received in revised form 21 May 2020; Accepted 24 May 2020
Available online 28 May 2020
0960-894X/

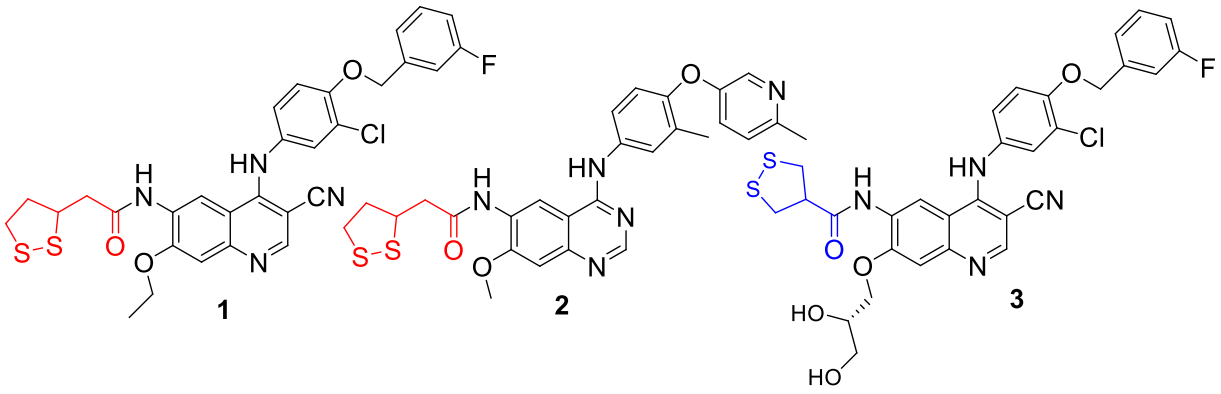

Fig. 1. Literature 1,2 dithiolanes.

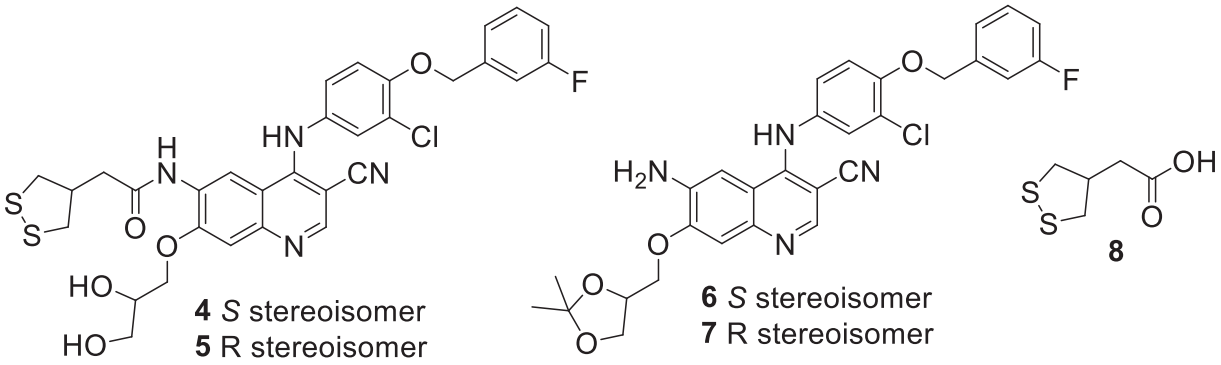

Fig. 2. Structures of target compounds **4** and **5** and intermediates **6–8.**

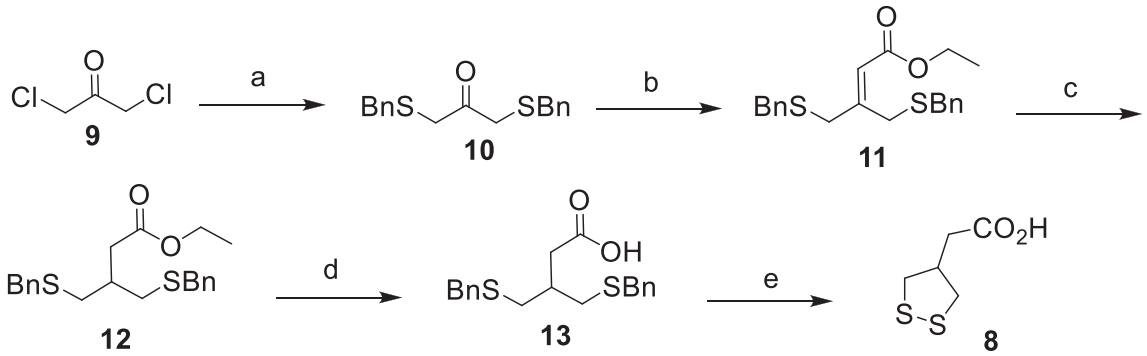

Scheme 1. Reagents and conditions: (a) EtOH 0 °C, BnSH, KOH, rt 2 h 44% (b) ethyl 2-(triphenylphosphanylidene)acetate $PPh_3 = CHCO_2Et$, toluene 120 °C, 81% (c) THF-MeOH 1-4, $NaBH_4$, $NiCl_2.6H_{2O}$ rt 2 h 35% (d) 10% NaOH 50 °C 2 h 93% (e) Liquid ammonia, toluene −78 °C, O_2 2 h 85%.

We have focused our biochemical SAR on the EGF family of kinases based on our earlier findings where high selectivity of **1** over the TEC family kinases was realized.[2] Our primary assay was the radioisotope filter binding (RFB) assay.[3] This assay is an activity-based platform that has the advantage of directly detecting the true catalytic product. Kinase profiling experiments were run at 10 μM ATP concentration relative to staurosporine as a positive control. To our delight, analogs **3–5** displayed potent inhibitory activities against the EGF family, in particular, against $EGFR^{WT}$ and Her4 (ErbB4) with **4** being *ca.*10 fold most potent against Her4 having an IC_{50} value of 0.03 nM (Table 1). In fact, all three compounds **3–5** display potent activity against Her4 over $EGFR^{WT}$ based on the IC_{50}s ratio range of 3.3–80 (Table 1). Comparison of the kinase profile of **4** to the clinically used drug, lapatinib indicates that both inhibitors have similar potency against $EGFR^{WT}$, however, lapatinib[4] is 13-fold more potent than **4** against Her2 whereas **4** is more potent against Her4 with an IC_{50} ratio of $EGFR^{WT}$/Her4 of 80 for **4** versus 0.008 for lapatinib (Table 1).

Next, we evaluated the inhibition data against mutant EGFR ($EGFR^{L858R}$, $EGFR^{L858R/T790}$ and $EGFR^{ex19del}$) relative to lapatinib. The data in Table 2 indicates reduced potency of **3–5** against this set of mutant enzymes compared to the wild type enzyme with *ca.* a 10-fold loss of activity between **3** and either **4** or **5** against $EGFR^{L858R}$ or $EGFR^{ex19del}$ mutant (Supplementary Table 1). Although inhibitor **3** displays greater potency against these mutant enzymes, it also exhibits appreciable potency against $EGFR^{WT}$ possibly due to the methylene spacer between **3** and either **4** or **5** affecting its binding mode.[1,11] In a similar manner to lapatinib, none of the inhibitors exhibited appreciable activity against the double mutant $EGFR^{L858R/T790}$. Therefore, it was concluded from the data in Tables 1 and 2 that the biochemical profile of **4** is best described as a dual potent inhibitor of $EGFR^{WT}$/Her4 with moderate activity against Her2 and weaker activity against activating EGFR mutations. Lapatinib on the other hand is a dual $EGFR^{WT}$/Her2 inhibitor with weak activity against Her4.

To set the potent Her4 kinase inhibition finding of **4** in context,

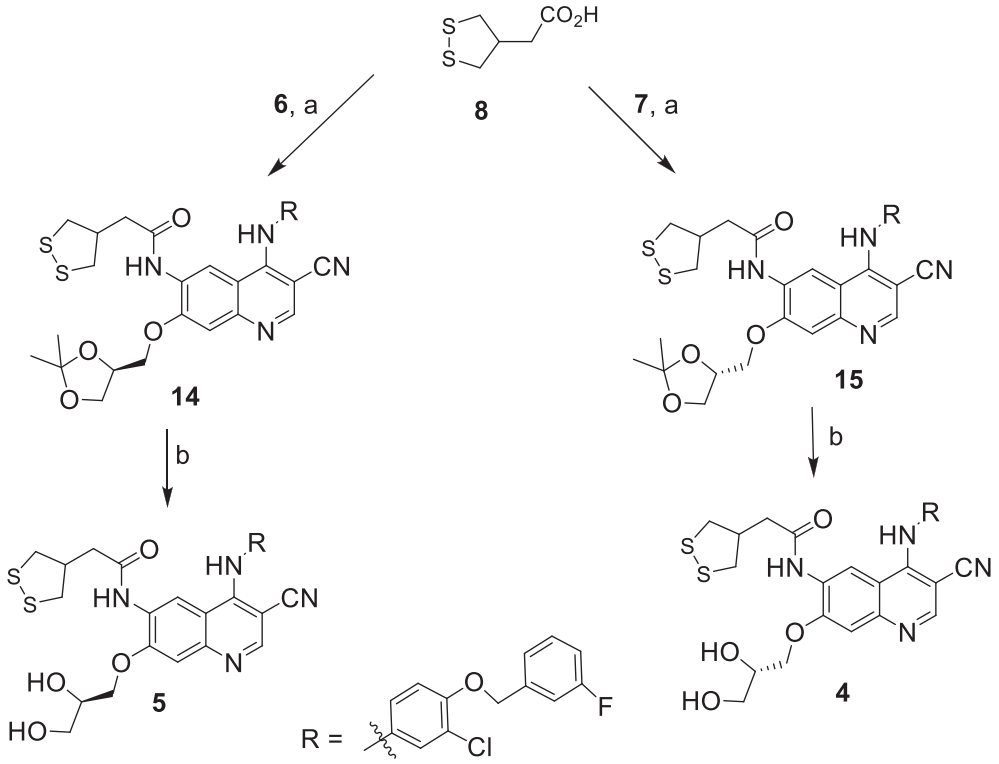

Scheme 2. Reagents and conditions: (a) NMP, EDC 90 °C 12 h, HPLC 23–36% (b) HCL MeOH rt 0.5 h, 80–98%.

Table 1
SAR in radioisotope filter binding assay (IC_{50} Values in nM).*

Entry	Compound	$EGFR^{WT}$	Her2	Her4	Ratio**
1	3	1.5	167	0.45	3.3
2	4	2.4	121	0.03	80
3	5	2.0	104	0.19	10.5
4	Lapatinib[4]	3.0	9.2	387	0.008
5	Staurosporine	125	104	535	4.3

*Ten point dose response curve, **IC_{50} values ratio of $EGFR^{WT}$/Her4.

Table 2
Kinase profile in mutant EGFR (IC_{50} Values in nM).*

Entry	Compound	$EGFR^{WT}$	$EGFR^{L858R}$	$EGFR^{L858/T790M}$	$EGFR^{ex19del}$
1	3	1.5	51	> 10,000	204
2	4	2.4	419	> 10,000	1990
3	5	2.0	387	NT	1280
4	Lapatinib[4]	3.0	8.0	> 4,000	NA
5	Staurosporine	125	58.7	2.3	41

*Ten point dose response curve. NT not tested, NA not available

comparison with earlier analogs[2] indicates a substantial increase in potency of **3–5** against Her4 in the RFB assay. For example, further comparison between **3, 5** and **16** (Fig 3) which lacks the C_7 substituent,[2] reveals over 9400-fold increase in potency (Supplementary Table 2). against Her4 (IC_{50} 0.03 versus 284). The C_7 dihydroxy-propoxy and the C_6 2-(1,2 dithiolan-4-yl)acetamide substituents, in concert together, appear to be responsible for this dramatic finding. Interestingly, in the case of the covalent inhibitors, afatinib and **17**, C_7 modifications with either (*S* 7-tetrahydrofuran-3-yl)oxy or (6-methyl-6-azaspiro[2.5]octan-1-yl)ethoxy substituents have also resulted in potent Her4 biochemical activities of 1.0 and 1.2 nM respectively.[5,6]

Whilst inhibitor **4** has comparable activity to gefitinib, lapatinib and afatinib against EGFR, it exhibits weaker activity than the latter two inhibitors against Her2 (Supplementary Table 3). The kinase profile of **4** bears some resemblance to lapatinib, the greatest differentiation of **4** relates to its superior activity against Her4 and weaker activity against Her2 (Supplementary Table 3).

Although the RFB assay was our primary biochemical assay, **4** was further evaluated for EGFR and Her4 inhibition in various assay platforms, specifically in the CaPBA (Carna Kinase Probe for Binding Assay) competitive binding assay[7] which measures interactions in the inactive state of the kinase and the KINOME*scan*™ competition binding assay,[8]

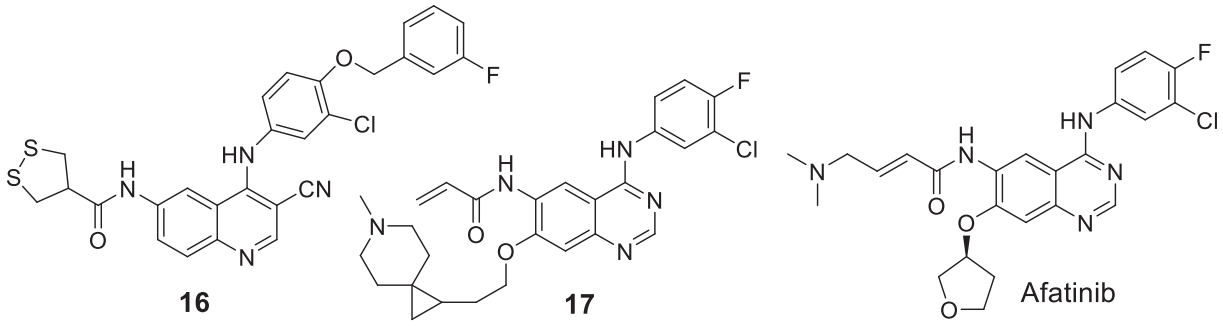

Fig. 3. Structures of Inhibitors **16**, **17** and afatinib.

Table 3
Comparative inhibition (in nM) of **4** relative to reference compounds.

Entry	Kinase	RFB[a]	CaPBA[a]	KINOME*scan*™ [b]
1	$EGFR^{WT}$	2.4/125	12.3/50.5	NT
2	$EGFR^{L858R}$	419/58.7	18.1/12.6	9.2/2.8
3	Her2	121/104	112/131	NT
4	Her3	NA	NA	380
5	Her4	0.03/535	12.2/29.4	6/54

[a]IC_{50} **4**/ IC_{50} staurosporine, [b] K_d **4**/K_d lapatinib, NA not available, NT not tested.

that quantitatively measures the ability of a compound to compete with an immobilized, active-site directed ligand. Despite the good potency of **4** against Her4 in these two assays relative to reference compounds, the potent picomolar inhibition of Her4 seen in the RFB assay was reduced in these assays (Table 3). Moreover, variations in the degree of $EGFR^{L858R}$ inhibition between the RFB and the other two assays were noted (IC_{50} 419 vs 18.1, 9.2 nM) while inhibition studies of $EGFR^{WT}$ and Her2 (ErbB2) kinases revealed no appreciable differences in the inhibition profile. Furthermore, **4** inhibited Her3 (ErbB3) with a K_d value of 380 nM (Table 3). These data highlight the need for care in comparing kinase assay data between different platforms due to recombinant kinases used, inhibition of active versus inactive kinases, assay conditions, ATP concentrations and format.

The clinical benefits of inhibiting both wild type and mutant EGFR and Her2 are now clearly established.[1] Disease prognosis associated with ErbB inhibition often reflects functional interdependency among these receptors which impact signaling pathways.[9] In several cancers, the role of Her4 inhibition is now being recognized. In breast cancer cells, Her4 signaling promotes differentiation and growth inhibition and loss of Her4 expression is a marker for resistance to tamoxifen.[9] Molecular alterations in esophageal and head-and-neck squamous cell carcinomas cell lines overexpressing Her4 are hypersensitive to afatinib.[10] These cell lines harbor an Her4 G1109C mutation which is an activating oncogenic mutation with a transformational ability and tumorigenicity.[10] The addiction of cancer cells to activating mutations in EGFR for proliferation suggests that targeted therapy with Her4 inhibitors may have future value in certain breast, esophageal and head-and-neck squamous cell carcinomas.

Structural studies of ErbBs have established a molecular basis for understanding many aspects of their functional signaling.[1,11] Active ErbB kinases, due to phosphorylation of tyrosine residues, bind ATP which results in several conformational changes including 1) relative orientation of N- and C-terminal lobes, 2) disposition of the activation loop (DFG) 3) orientation of the αC helix and 4) electrostatic switch where the β3 lysine salt bridge with the DFG-D residue in the inactive form switches to a salt bridge between the β3-lysine and the αC-glutamate with the concomitant formation of the αC-in conformation. This knowledge has aided in the design of small molecule inhibitors of ErbB family targeting certain protein sites. Thus, inhibitors are classified as type I when they bind within the adenine-binding pocket of an active protein kinase,[12,13] type II inhibitors bind to an inactive kinase with the DFG-D out motif[12,13]; type III inhibitors[12–14] bind in an allosteric site between the *N*-terminal and C-terminal lobes; type IV bind in an allosteric site outside of the adenine-binding pocket[12,14]; type V are bivalent inhibitors that span two distinct parts of the protein kinase domain[15] and type VI are covalent inhibitors.[16]

To date there are no structural data of **4** bound to either Her4 or EGFR. However, since **4** has an anilino substituent similar to that of lapatinib and a core 3-cyanoquinoline similar to neratinib but different C_6 and C_7 substituents, the reported x-ray crystallographic structural information from lapatinib and neratinib bound to EGFR and Her4 are relevant to **4**. Lapatinib inhibits Her4 with an IC_{50} of 367[17] or 1400 nM.[18] It binds to the inactive form of Her4 (PDB code: 3BBT, 2.8 Å) and EGFR (PDB code: 1XKK, 2.4 Å) in the same binding site

Table 4
Cellular activity of **4** and **5** (nM) in select cells in the NCI-60 Panel[a].

Cell Line	Origin/Disease	**4**		**5**	
		GI_{50}	TGI	GI_{50}	TGI
CCRF-CEM	Leukemia/ALL[b]	42	146	112	283
K-562	Leukemia/CML[c]	94	208	148	454
MOLT-4	Leukemia/ALL[b]	74	175	93	209
SR	Leukemia/Large cell	66	246	132	608
NCI-H460	NSCLC/Carcinoma	103	263	128	312
NCI-H226	NSCLC/Adenocarcinoma	198	883	690	1830
MCF7	Breast/Adenocarcinoma	86	182	91	193
MDA-MB-231	Breast/Adenocarcinoma	103	237	208	722
MDA-MB-468	Breast/Adenocarcinoma	70	155	120	385
HS 578 T	Breast/Carcinoma	105	282	512	1740
PC-3	Prostate/Adenocarcinoma	89	204	174	455
DU-145	Prostate/Carcinoma	134	424	637	1365
HCT-116	Colon/Adenocarcinoma	88	204	98	209
M14	Malignant melanoma	83	251	141	482
SK-MEL-28	Malignant melanoma	63	136	129	350
SF-268	Anaplastic astrocytoma	83	778	404	1325

[a]Five dose response curve, each value is an average of 2 experiments; [b] Acute lymphoblastic leukemia, [c] Chronic myelogenous leukemia. https://dtp.cancer.gov/services/nci60data/meangraph/gi50/jpg/-4.0/715055.

interacting with residues in the front pocket, gate area, and back pocket.[18] The difference between the binding mode of lapatinib between EGFR and Her4 is a flip in the fluorophenyl ring, which alters the position of the fluorine but does not introduce or break contacts with residues not found in both EGFR and Her4.[18] Likewise, the structure of neratinib bound to a mutant EGFR (PDB code: 3W2Q, 2.2 Å) shows that it binds to an inactive form of the enzyme spanning the front pocket, gate area and back pocket.[19] It is possible, based on these precedents[18,19] that **4** engages the inactive form of EGFR/Her4 but the specific amino acids residues that contact the novel C_6 and C_7 substituents remain to be determined.[20,21]

Next, the cellular activity of **4** and **5** was evaluated in the NCI-60 panel and reported in Table 4 as GI_{50} (the concentration of the drug causing 50% growth inhibition) and TGI (the total growth inhibition) values in nM. Compound **4** has consistently, albeit marginally better activity over **5** particularly in a select set of cell lines from the leukemia, breast, NSCLC and prostate panels. This trend was also noted in colon, melanoma and CNS lines. The GI_{50} values range for **4** are between 42 and 198 nM for the 17 cell lines shown in Table 4 and the TGI data are $<$ 300 nM in all cell lines shown in Table 4 except for three lines (NCI-H226, DU-145 and SF-268). The LC_{50} values measuring the cytotoxic concentration are $>$ 375 nM resulting in therapeutic indices ($TI = LC_{50}/GI_{50}$) of $>$ 4 as listed in Supplementary Table 4.

Furthermore, based on the data in Table 4, we choose to profile **4** in three cell lines (MOLT-4, NCI-H460 and HCT-116) in the hollow fiber assay[22] using the ProQinase protocol (ProQinase Reaction Biology, GmbH, Freiburg, Germany) in female NMRI nude mice with the objective of selecting one or more cell lines for future xenograft studies. The study design used 12 animals for vehicle (5% DMSO, 5% DMA, 20% PEG400, 40% PG, 30% PBS) and testing with dosing over 14 days at 10 mpk. All 12 animals (vehicle and test) exhibited no signs of toxicity or body weight loss during the 14 day period. Inhibitor **4** (SAB402, NSC code: D-787238) reduced cell viability using CellTiter-Glo® in the intraperitoneally implanted hollow fibers which have been loaded with MOLT-4 cells in a statistically very significant manner ($p = 0.0062$) when compared to vehicle (Fig 4). Similarly, as shown in Fig 4 significant reduction in cell viability was obtained in the H460 cells ($p = 0.0116$), whereas the HCT-116 cells group showed no significant reduction of cell viability. No substantial effects were observed in the sc compartment in all three cell lines.

In conclusion, we have developed a synthetic protocol to 2-(1,2-dithiolan-4-yl)acetic acid **8** for use to prepare target novel 3-

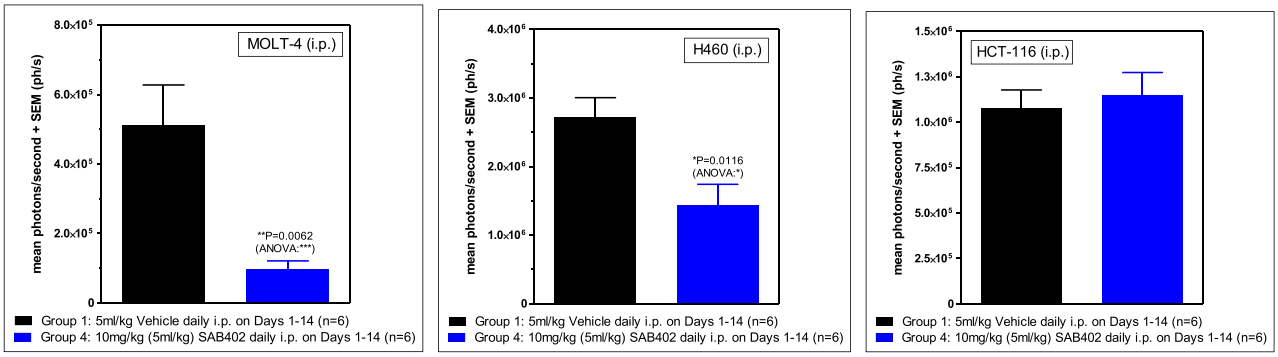

Fig. 4. Cell Viability (CellTiter-Glo®) in the *i.p.* Implanted MOLT-4 (right), NCI-H460 middle and HCT-116 (left) Hollow Fibers.

cyanoquinolines **4** and **5** as inhibitors of the EGF family. From a SAR perspective in the RFB assay, the methylene spacer in **4** and **5** as compared to **3**, has resulted in maintaining potency against $EGFR^{WT}$, slightly increased Her2 activity but decreased the selectivity towards activating mutations of EGFR ($EGFR^{L858R}$, $EGFR^{ex19del}$). Importantly, whilst all inhibitors **3–5** displayed potent Her4 inhibition with IC_{50} values in the range of 0.03–0.45 nM, dual EGFR/Her4 activity ratio was the highest with **4** in the RFB assay. Preference for the *S* stereochemistry was established in parallel to that in the asparagusic acid series.[2] The Her4 inhibition was reduced in two competitive binding assays. Inhibitor **4** was also found to be marginally but consistently more potent than **5** in the NCI-60 cellular assays across various panels notably select cells from leukemia, NSCLC, breast, prostate, colon and CNS lines. In the hollow fiber assay using NMRI nude mice, **4** reduced cell viability using CellTiter-Glo® in the intraperitoneally implanted hollow fibers which have been loaded with MOLT-4 and NCI-H460 cells in a statistically very significant and significant manner but had no effect in the HCT116 group.

Declaration of Competing Interest

The authors declare that they have no known competing financial interests or personal relationships that could have appeared to influence the work reported in this paper.

Acknowledgements

We thank the NCI DTP program (Bethesda, MD, USA) for cellular data, and Cynthia Obodozie (ProQinase, Freiburg, Germany) for the Hollow Fiber Assay data, Reaction Biology Corporation (Malvern, PA, USA), Eurofins (San Diego, CA, USA) and CarnaBio (MA, USA) for all biochemical data. We also thank Mallaiah Keesara for HPLC analyses, Vijay Potluri, Pranab Maiti, Mahdi B. Fawzi and John O'Connell for useful discussions on this research. This paper is dedicated with appreciation to Magid Abou-Gharbia Moulder Center for Drug Discovery, Temple University, PA, USA.

This research did not receive any specific grant from funding agencies in the public, commercial, or not-for-profit sectors

Appendix A. Supplementary data

Supplementary data to this article can be found online at https://doi.org/10.1016/j.bmcl.2020.127288.

References

1. Roskoski Jr R. Small molecule inhibitors targeting the EGFR/ErbB family of protein tyrosine kinases in human cancers. *Pharmacol Res.* 2019;139:395–411. https://doi.org/10.1016/J.phrs.2018.11.014.
2. Mansour TS, Pallepati RR, Basetti V, et al. Lead generation of 1,2 dithiolanes as exon 19 and exon 21 mutant EGFR tyrosine kinases inhibitors. *Bioorg Med Chem Lett.* 2019;29:1435–1439. https://doi.org/10.1016/j.bmcl.2019.04.029.
3. Wang Y, Ma H. Protein kinase profiling assays: a technology review. *Drug Discover Today Technol.* 2015;18:1–8. https://doi.org/10.1016/j.ddtec.2015.10.007.
4. D. Li L. Ambrogio T. Shimamura et al. BIBW2992, an irreversible EGFR/HER2 inhibitor highly effective in preclinical lung cancer models Oncogene 27 2008 4702 4711 10:1038/onc.2008.109.
5. Solca F, Dahl G, Zoephel A, et al. Target binding properties and cellular activity of afatinib (BIBW 2992), an irreversible ErbB family blocker. *J Pharmacol Exp Ther.* 2012;343:342–350. https://doi.org/10.1124/jpet.112.197756.
6. Zhenhua H, Yanyan D. Preparation of quinazoline derivatives as antitumor agents PCT Int. Appl. (2012), WO 2012027960 A1 20120308.
7. https://www.carnabio.com/english/discovery/platform.html.
8. Karaman MW, Herrgard S, Triber DK, et al. Quantitative analysis of kinase inhibitor selectivity. *Nat Biotechnol.* 2008;26:127–132.
9. Koutras AK, Fountzilas G, Kalogeras KT, et al. The upgraded role of Her3 and Her4 receptors in breast cancer. *Critical Rev Oncol/Hematol.* 2010;74:73–78. https://doi.org/10.1016/j.critrevonc.2009.04.011.
10. Nakamura Y, Togashi Y, Nakahara H, et al. Afatinib against esophageal or head-and-neck squamous cell carcinoma:significance of activating oncogenic *HER4* mutations. *Mol Cancer Ther.* 2016;15:1988–1997. https://doi.org/10.1158/1535-7163.MCT-15-0737.
11. Bikker JA, Brooijmans N, Wissner A, Mansour TS. Kinase domain mutations in cancer: implications for small molecule drug design strategies. *J Med Chem.* 2009;52:1493–1509. https://doi.org/10.1021/jm8010542.
12. Zuccotto F, Ardini E, Casale E, Angiolini M. Through the "gatekeeper door": exploiting the active kinase confirmation. *J Med Chem.* 2010;53:2691–2694. https://doi.org/10.1021/jm901443h.
13. Dar AC, Shokat KM. The evolution of protein kinase inhibitors from antagonists to agonists of cellular signaling. *Ann Rev Biochem.* 2011;80:769–795. https://doi.org/10.1146/annurev-biochem-090308-173656.
14. Gavrin LK, Saiah E. Approaches to discover non-ATP site inhibitors. *Med Chem Commun.* 2013;4:41.
15. Lamba V, Ghosh I. New directions in targeting protein kinases: focusing upon true allosteric and bivalent inhibitors. *Curr Pharm Design.* 2012;18:2936–2945. https://doi.org/10.2174/138161212800672813.
16. R. Roskoski Jr. Classification of small molecule protein kinase inhibitors based upon the structures of their drug-enzyme complexes Pharmacol. Res. 2016;103:26–48. https: //doi.org/10.1016/j.phrs.2015.10.021.
17. Ruznak DW, Lackey K, Affleck K, et al. The effects of the novel, reversible epidermal growth factor receptor/ErbB-2 tyrosine kinase inhibitor, GW2016, on the growth of human normal and tumor-derived cell lines in vitro and in vivo. *Mol Cancer Ther.* 2001;1:85–94.
18. Qiu C,Tarrant MK, Choi SH, et al. Mechanism of activation and Inhibition of the HER4/ ERBB4 Kinase. Structure 2008;16:460 – 467. DOI.10.1016/j.str.2007.12.016.
19. Sogabe S, Kawashita Y, Igaki S, et al. EGFR kinase domain T790/L858R mutant with HKI-272. *ACS Med Chem Lett.* 2013;4:201–205. https://doi.org/10.1021/ml300327z.
20. Topol IA, Nemukhin AV, Chao M, et al. Quantum chemical studies of reactions of the cyclic disulfides with the zinc finger domains in the HIV-1 nucleocapsid protein (NCp7). *J Am Chem Soc.* 2000;122:7087–7094. https://doi.org/10.1021/ja000585x.
21. Beno BR, Yeung K-S, Bartberger MD, Pennington LD, Meanwell NA. A survey of the role of noncovalent sulfur interactions in drug design. *J Med Chem.* 2015;58:4383–4438. https://doi.org/10.1021/jm501853m.
22. Sinz A, Siedentopf O, Leisegang U, Ruf S, Bijelic G, Weber H, Obodozie C. Evaluation of hollow fiber model as a highly predictive in vivo testing system for the selection of xenograft tumor models in cancer drug discovery. AACR-NCI-EORTC International Conference on molecular targets and cancer therapeutics: discovery, biology and clinical applications October 26-30, 2017. Philadelphia, PA, U.S.A. Poster A014.